ISSN 1061-9348, Journal of Analytical Chemistry, 2024, Vol. 79, No. 9, pp. 1338–1344. © Pleiades Publishing, Ltd., 2024.

ARTICLES

Determination of Hydrogen Sulphide in Air with an Indium Oxide Semiconductor Sensor

A. V. Shaposhnik[a], *, A. A. Zviagin[a], and S. V. Ryabtsev[b]

[a] *Voronezh State Agrarian University, Voronezh, 394087 Russia*

[b] *Voronezh State University, Voronezh, 394018 Russia*

**e-mail: a.v.shaposhnik@gmail.com*

Received April 4, 2024; revised April 4, 2024; accepted April 4, 2024

Abstract—Hydrogen sulfide, a toxic gas, can be released into the air during oil and natural gas extraction, metallurgical production, and the storage and processing of industrial and household wastes. The determination of hydrogen sulfide in the atmosphere is a pertinent task in analytical chemistry. The established methods, such as chromatography or mass spectrometry, are unsuitable for continuous monitoring in hard-to-reach places. This creates a practical need for a low-cost chemical sensor that offers high sensitivity and selectivity. In this study, gas-sensitive materials based on In_2O_3 with catalytic additives—primarily palladium (as PdO) and silver (as Ag_2O)—were synthesized. The synthesis proceeded in several stages. Initially, an $In(OH)_3$ sol was prepared, followed by centrifugation and thermal treatment to yield indium oxide nanopowder. The material was characterized by transmission electron microscopy (TEM) and X-ray powder diffraction. Subsequently, the indium oxide nanopowder was blended with catalytic additives and a binder to form a paste. The gas-sensitive material was obtained by annealing the paste at 750°C. The sensor properties of these gas-sensitive materials were investigated with respect to hydrogen sulfide and carbon monoxide under nonstationary temperature conditions: heating to 450°C for 2 s and cooling to 100°C for 13 s. The study demonstrated that nanodispersed indium oxide-based materials exhibit high sensitivity to hydrogen sulfide and exceptional selectivity.

Keywords: metal oxide sensors, hydrogen sulfide, indium oxide synthesis, characterization of indium oxide, sensitivity, nonstationary temperature mode

DOI: 10.1134/S1061934824700709

Hydrogen sulfide is a metabolic product and performs several vital functions in a body. However, it is also a potent neuroparalytic poison. Inhalation of hydrogen sulfide in concentrations of 1–10 ppm can cause dizziness, headache, nausea, and vomiting. In concentrations of 10–100 ppm, hydrogen sulfide can lead to coma, seizures, and pulmonary edema. Concentrations of hydrogen sulfide in air above 100 ppm can lead to rapid poisoning: seizures and the loss of consciousness can quickly progress to respiratory arrest and death.

Hydrogen sulfide has strong odor; however, when inhaled in sufficiently high concentrations, the paralysis of the olfactory nerve causes the odor to become almost immediately undetectable.

Hydrogen sulfide is present in natural gas and associated petroleum gases, sometimes in significant quantities. It also forms in metallurgy and during the storage and processing of industrial wastes. Additionally, hydrogen sulfide is released during the decay of proteins [1].

The task of determining low concentrations of hydrogen sulfide in the air is crucial due to the risk of poisoning to humans. Hydrogen sulfide also serves as a biomarker for the body's condition. Furthermore, hydrogen sulfide detection can be used to monitor the quality of food products.

There are methods of gas analysis that combine high sensitivity and selectivity, such as gas chromatography, mass spectrometry, and chromatography–mass spectrometry. However, these instruments are not only highly expensive but also require highly qualified maintenance. For the continuous monitoring of the atmosphere in hard-to-reach places, there is a need in developing compact and affordable gas analyzers based on chemical sensors. For hydrogen sulfide detection, semiconductor or electrochemical sensors can be used. Semiconductor sensors offer advantages over electrochemical ones due to their lower cost and capability of continuous operation over extended periods.

The sensor response in semiconductor metal oxide sensors is associated with changes in electrical conductivity due to redox reactions on the surface. Gas-sensitive materials of specific compositions, such as copper or silver oxides, are commonly used for hydrogen sulfide detection. This is because hydrogen sulfide

adsorption can lead not only to its oxidation to sulfur oxides but also to changes in the phase composition and the reversible transformation of oxides into sulfides, exhibiting high electrical conductivity. This process can additionally contribute to the sensor response. For instance, additives of copper (+2) oxide lead to changes in the composition of the gas-sensitive layer upon hydrogen sulfide adsorption [2, 3].

The most common material for hydrogen sulfide sensors is tin dioxide doped with copper (+2) oxide additives. High sensitivity and selectivity have been demonstrated, particularly in electrospun nanofibers of SnO_2 coated with CuO [4, 5]. Sensors for H_2S have been developed based on SnO_2 nanowires coated with CuO nanoparticles [6, 7], and the sensor response mechanism of SnO_2:CuO thin films produced by thermal spraying has been investigated [8]. A gas-sensitive material based on hollow nanospheres coated with CuO has been successfully used for hydrogen sulfide detection in medical diagnostics [9]. A multilayer structure SnO_2–CuO showed response of more than four orders of magnitude for 20 ppm H_2S with low response times [10]. The influence of the mutual diffusion of SnO_2 and CuO nanoparticles on the sensor properties to hydrogen sulfide has been examined [11]. Sensor properties of thin-film nanostructures based on CuO/SnO_2 have also been studied [12]. However, the most common method for fabricating SnO_2/CuO nanocomposites is the sol–gel process [13].

In addition to copper oxide additives, sensors for hydrogen sulfide detection also contain silver additives. Similar to copper oxide, silver oxide can reversibly transform into silver sulfide, which exhibits high electrical conductivity. The conversion of silver oxide to silver sulfide significantly contributes to the analytical signal of the sensor [14, 15]. Adding silver to nanocrystalline SnO_2 enhances response to hydrogen sulfide [16–18].

For hydrogen sulfide detection, pure SnO_2 has been employed [19], as well as SnO_2 with additives of platinum [20] or fullerenes [21].

Copper oxide in some cases serves as a basic material for the sensor itself rather than as an additive to other metal oxide materials. For instance, a highly sensitive sensor has been developed based on palladium-doped CuO nanoflowers [22]. The sensor properties of unsintered nanowires of copper (+2) oxide have been investigated [23].

It is known that in going from typical stationary temperature modes to nonstationary ones, a significant increase in sensitivity in often observed [24]. As demonstrated in this study, the use of nonstationary temperature conditions also enhances the selectivity of hydrogen sulfide determination.

EXPERIMENTAL

A 1.25-g weighed portion of indium nitrate (CAS no. 207398-97-8; $InN_3O_9{\cdot}n$HOH, Sigma-Aldrich) was dissolved in 250 mL of glacial acetic acid. A 25% aqueous solution of ammonia was added dropwise to the resulting solution, cooled to 8–10°C, until reaching the isoelectric point of indium hydroxide (pH 6),

$$2In^{3+} + 6NH_3{\cdot}HOH(aq) \rightarrow In_2O_3{\cdot}3HOH\downarrow + 6NH_4^+(aq). \quad (1)$$

Ammonia was added dropwise with continuous stirring, and the temperature of the reaction mixture was maintained at 8–10°C throughout. The precipitated indium hydroxide gel was separated by centrifugation. The supernatant solution was decanted, and the precipitate with the remaining solution residues was transferred to an evaporation dish and dried at 80°C for 12 h. The dried material was then calcined for 8 h at 300°C (sample 1) and additionally for 6 h at 500°C (sample 2). As a result of the calcination process, indium oxide powder was obtained.

$$In_2O_3{\cdot}3HOH \rightarrow In_2O_3 + 3H_2O. \quad (2)$$

The obtained indium oxide powder was examined by transmission electron microscopy (Fig. 1). Samples of In_2O_3, obtained at calcination temperatures of 300°C and 500°C, were characterized by X-ray powder diffraction (XRD) using a DRON-4 diffractometer with a copper anode. The diffraction patterns were analyzed using the Powder Diffraction File (PDF-2) database. An analysis of the diffraction patterns revealed that both samples (300 and 500°C) exhibited cubic crystal structures. On the left ordinate axis of Fig. 2, data from the PDF cards for cubic-phase In_2O_3 are plotted, while on the right ordinate axis, experimental XRD data are presented.

To create a gas-sensitive layer based on indium oxide with silver oxide additives, the indium oxide powder was treated with a solution of silver nitrate. After drying, terpineol was added to the powder as a binding component. The resulting paste was applied onto a dielectric substrate made of aluminum oxide, featuring specialized platinum electrodes for conductivity measurements and a platinum heater. The substrate with the applied paste was heated to 750°C, during which the binding component was burned off, leaving a gel of indium oxide with silver additives.

A gas-sensitive layer based on indium oxide with palladium oxide additive was prepared using a similar procedure, in which the indium oxide powder was treated with a solution of tetraammine palladium(II) nitrate instead of silver nitrate.

To assess the sensor properties of the resulting materials, verification gas mixtures “hydrogen sulfide in synthetic air” and “carbon monoxide in synthetic air” were used in concentrations of 10 and 200 ppm, respectively, diluted with synthetic air. The total flow

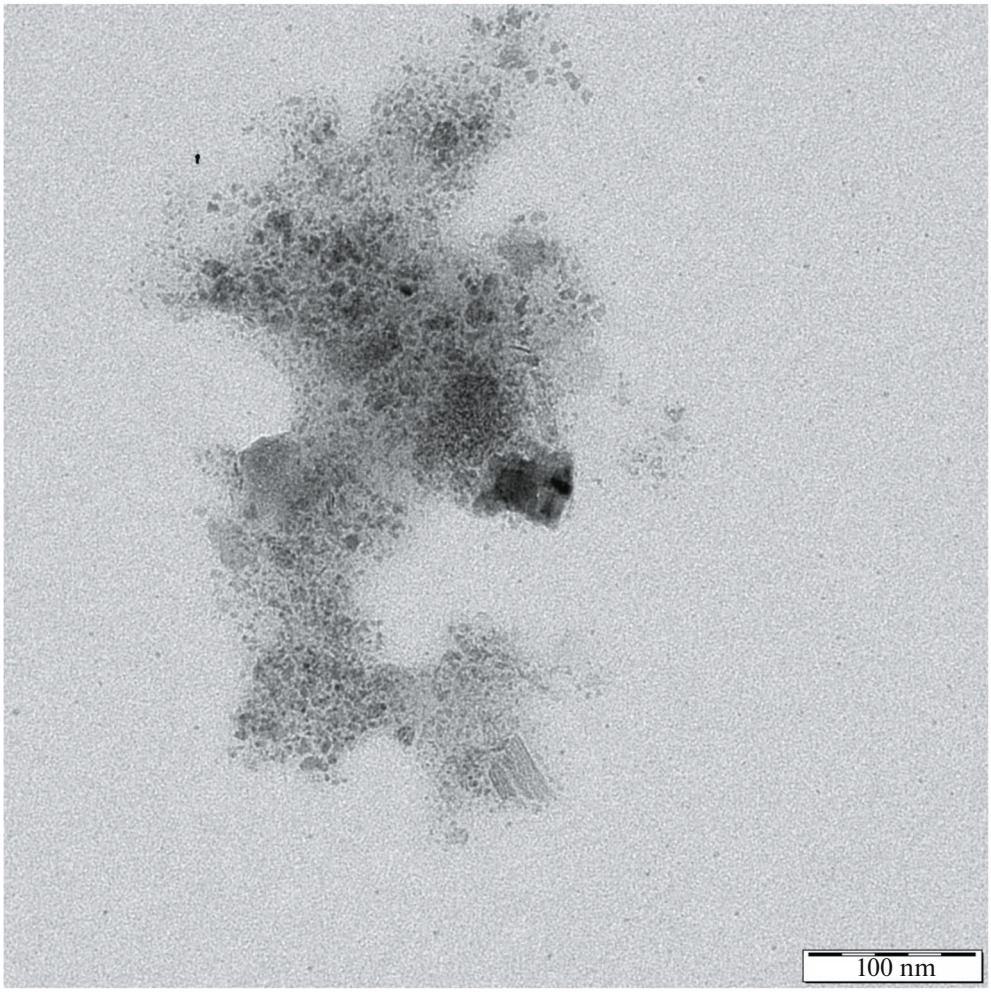

Fig. 1. A TEM image of indium oxide powder particles.

rate was maintained at 250 mL/min. The sensor, housed in a TO-8 metallic package, was placed inside a stainless steel chamber. Its temperature was controlled using a special electronic device based on the temperature coefficient of the resistance of the heater, determined in preliminary measurements.

The electrical resistance of the gas-sensitive layer was measured using a specialized electronic device with a frequency of up to 40 Hz, and the data were recorded as a computer file. Each measurement cycle lasted 15 s, which consisted of 2 s of heating from 100 to 450°C, followed by 13 s of cooling from 450 to 100°C. These heating–cooling cycles were conducted continuously without interruption. Measurements from the first five cycles were discarded. For quantitative analysis, only one of the 575 points in each cycle was used, specifically at 14.95 s after the start of the cycle.

Response S was calculated as the ratio of electrical resistance R_0 in pure air to electrical resistance R_g in the investigated gas medium,

$$S = R_0/R_g. \quad (3)$$

RESULTS AND DISCUSSION

Figure 3 shows dependences of the electrical resistance of the In_2O_3–Pd sensor over time during one measurement cycle for different hydrogen sulfide concentrations. Increasing hydrogen sulfide concentration led not only to a significant increase in the sensor response but also altered the shape of the curves, particularly within the initial segment corresponding to heating the sensor from 100 to 450°C.

We obtained time dependences of the electrical resistance of the In_2O_3–Ag sensor during one measurement cycle for various concentrations of hydrogen sulfide (Fig. 4). The shape of the curves for the In_2O_3–Ag sensor (Fig. 4) differed significantly from those of the In_2O_3–Pd sensor (Fig. 3), indicating different mechanisms of chemisorption processes for different gas-sensitive materials not only in hydrogen sulfide media but also in air.

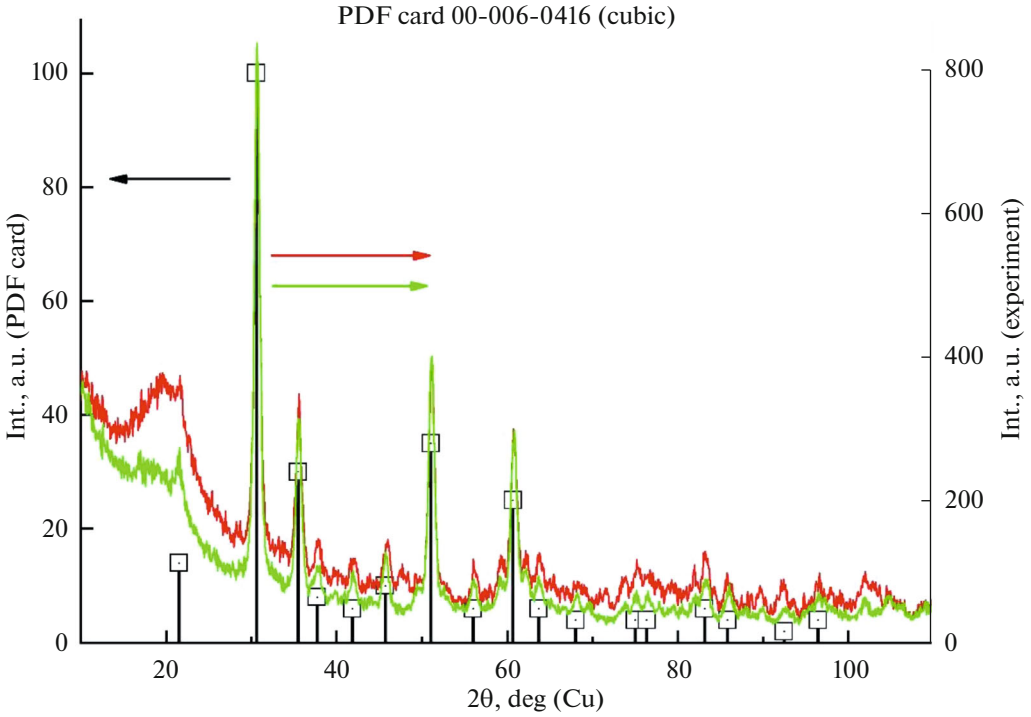

Fig. 2. X-ray powder diffraction of indium oxide powder.

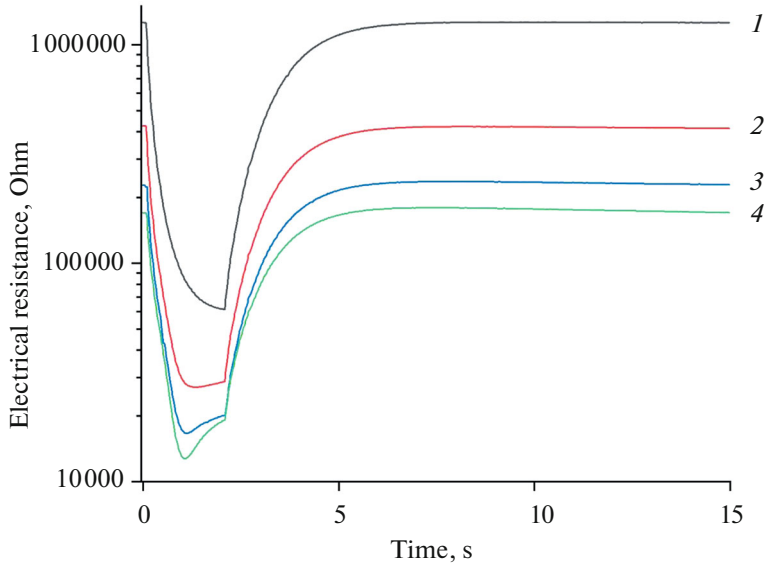

Fig. 3. Time dependence of the electrical resistance of an In_2O_3–Pd sensor during one measurement cycle with temperature ranging from 100 to 450°C: (*1*) synthetic air and (*2*) 5, (*3*) 20, and (*4*) 50 ppm H_2S.

To assess the selectivity of hydrogen sulfide detection, measurements were also conducted for carbon monoxide. Figure 5 illustrates time dependences of the electrical resistance of the In_2O_3–Pd sensor in one measurement cycle for different concentrations of carbon monoxide.

There are two approaches to the selective determination of gases using sensors. One approach involves the use of low-selectivity sensors, such as In_2O_3–Pd. The responses of this sensor in detecting carbon monoxide (Fig. 6, curve *2*) and hydrogen sulfide (curve *3*) are almost identical; however, the shapes of the curves

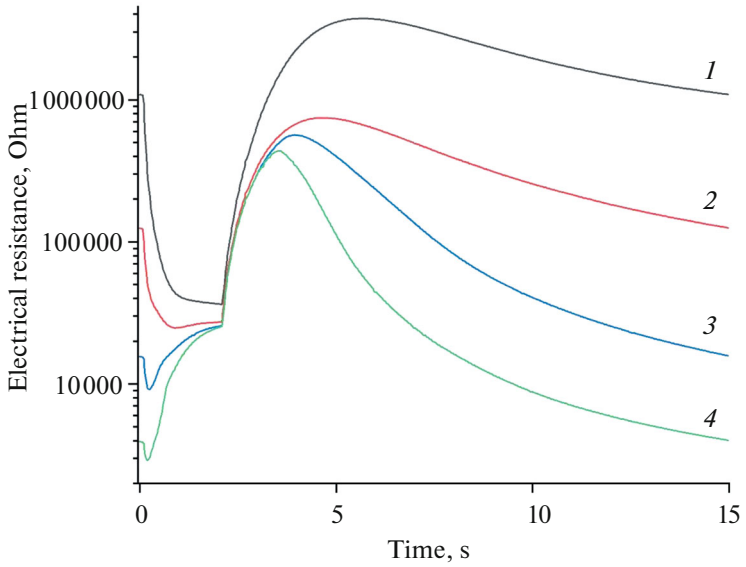

Fig. 4. Time dependence of the electrical resistance of In_2O_3–Ag sensor during one measurement cycle with temperature ranging from 100 to 450°C: (*1*) synthetic air and (*2*) 5, (*3*) 20, and (*4*) 50 ppm H_2S.

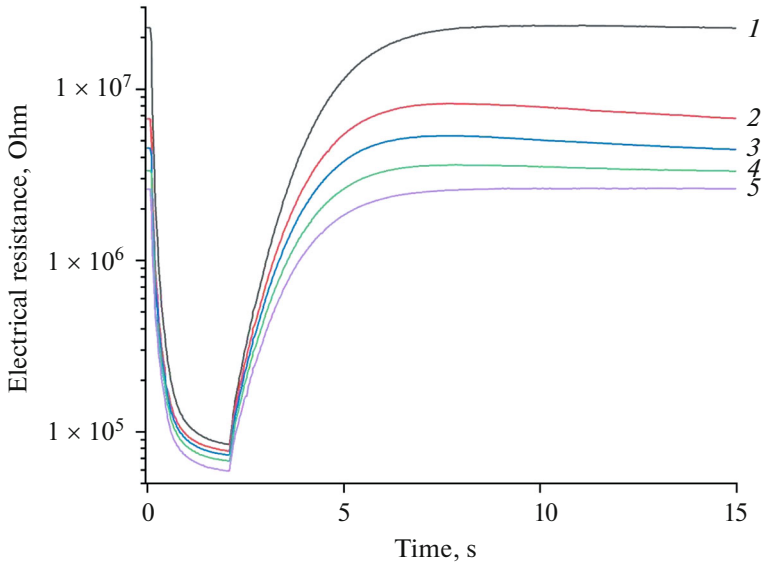

Fig. 5. Time dependence of the electrical resistance of In_2O_3–Pd sensor during one measurement cycle with temperature ranging from 100 to 450°C: (*1*) synthetic air and (*2*) 5, (*3*) 10, (*4*) 20, and (*5*) 50 ppm CO.

are different, particularly in the heating phase in the first two seconds (Figs. 3 and 5). The difference in the curve shapes offers a fundamental opportunity for selective analysis with the processing of the resulting multidimensional data arrays [24]. The qualitative and quantitative analysis of various gas media can thus be achieved using a single gas sensor. In this context, palladium is an optimal dopant for metal oxide semiconductors, such as SnO_2, ZnO, WO_3, or, as in this case, In_2O_3, because of its universal and highly effective catalytic properties.

However, there is another approach to achieving selective detection, based on the development of highly selective sensors. As shown in Fig. 6, the responses of the In_2O_3–Ag sensor in detecting hydrogen sulfide significantly exceed its responses in detecting carbon monoxide. Thus, the In_2O_3–Ag sensor can be used for the selective determination of hydrogen sulfide. This capability stems from the fact that, alongside the conventional mechanism involving a donor-type sensor response through redox processes on the surface, leading to a decrease in the electrical resis-

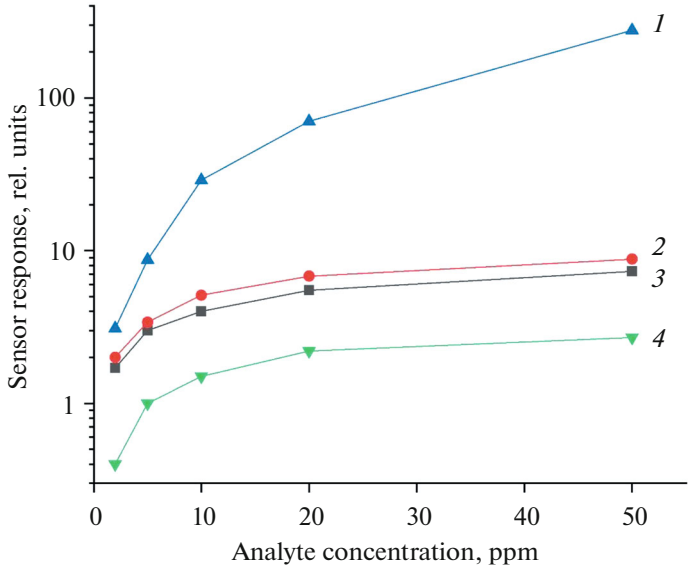

Fig. 6. Response dependences of (*1*, *4*) In_2O_3–Ag sensor and (*2*, *3*) In_2O_3–Pd sensor for (*1*, *3*) hydrogen sulfide and (*2*, *4*) carbon monoxide concentrations.

tance of an *n*-type semiconductor, an additional mechanism is implemented. This mechanism is induced by the reversible transformation of silver oxide into silver sulfide,

$$Ag_2O + H_2S \rightarrow Ag_2S + H_2O. \quad (4)$$

Silver sulfide possesses high electrical conductivity, thereby leading to an increase in the concentration of electrons throughout the gas-sensitive material (donor-type response).

CONCLUSIONS

Nanopowders of indium oxide were obtained by precipitation from a liquid phase followed by centrifugation, drying, and calcination. Subsequently, they were characterized by transmission electron microscopy and X-ray powder diffraction. Pastes were prepared from these nanopowders by adding catalysts (palladium and silver) along with a binding additive. Gas-sensitive layers (sensors) were formed by applying these pastes onto specialized dielectric substrates with electrodes and a heater, followed by calcination at 750°C.

The sensor material based on indium oxide with palladium additives exhibited high sensitivity to both hydrogen sulfide and carbon monoxide. In this scenario, the selectivity of an analysis can be achieved by analyzing the shapes of the obtained curves of electrical resistance over time.

The sensor material based on indium oxide with silver additives demonstrated high sensitivity to hydrogen sulfide and low sensitivity to carbon monoxide. In this case, the selective determination of hydrogen sulfide can be performed without complex mathematical processing of multidimensional data arrays.

FUNDING

The study was supported by the Russian Foundation for Basic Research, project no. 20-03-00901.

CONFLICT OF INTEREST

The authors of this work declare that they have no conflicts of interest.

REFERENCES

1. Guidotti, T.L., *Int. J. Toxicol.*, 2010, vol. 29, p. 569.
2. Maekawa, T., Tamaki, J., Miura, N., and Yamazoe, N., *Chem. Lett.*, 1991, vol. 20, no. 4, p. 575.
3. Tamaki, J., Maekawa, T., Miura, N., and Yamazoe, N., *Sens. Actuators, B*, 1992, vol. 9, no. 3, p. 197.
4. Choi, S.W., Zhang, J., Akash, K., and Kim, S.S., *Sens. Actuators, B*, 2012, vol. 169, p. 54.
5. Zhao, Y., He, X., Li, J., Gao, X., and Jia, J., *Sens. Actuators, B*, 2012, vol. 165, no. 1, p. 82.
6. Shao, F., Hoffmann, M.W.G., Prades, J.D., Zamani, R., Arbiol, J., Morante, J.R., Varechkina, E., Rumyantseva, M., Gaskov, A., Giebelhaus, I., Fischer, T., Mathur, S., and Hernández-Ramírez, F., *Sens. Actuators, B*, 2013, vol. 181, p. 130.
7. Hwang, I.S., Choi, J.K., Kim, S.J., Dong, K.Y., Kwon, J.H., Ju, B.K., and Lee, J.H., *Sens. Actuators, B*, 2009, vol. 142, no. 1, p. 105.
8. Katti, V.R., Debnath, A.K., Muthe, K.P., Kaur, M., Dua, A.K., Gadkari, S.C., Gupta, S.K., and Sahni, V.C., *Sens. Actuators, B*, 2003, vol. 96, nos. 1–2, p. 245.
9. Choi, K.I., Kim, H.J., Kang, Y.C., and Lee, J.H., *Sens. Actuators, B*, 2014, vol. 194, p. 371.

10. Verma, M.K. and Gupta, V., *Sens. Actuators, B*, 2012, vols. 166–167, p. 378.
11. Vasiliev, R.B., Rumyantseva, M.N., Podguzova, S.E., Ryzhikov, A.S., Ryabova, L.I., and Gaskov, A.M., *Mater. Sci. Eng., B*, 1999, vol. 57, no. 3, p. 241.
12. Vasiliev, R.B., Rumyantseva, M.N., Podguzova, S.E., Ryzhikov, A.S., Ryabova, L.I., and Gaskov, A.M., *Sens. Actuators, B*, 1998, vol. 50, no. 3, p. 186.
13. Malyshev, V.V. and Pislyakov, A.V., *Sens. Actuators, B*, 1998, vol. 47, nos. 1–3, p. 181.
14. Lantto, V. and Mizsei, J., *Sens. Actuators, B*, 1991, vol. 5, nos. 1–4, p. 21.
15. Harkoma-Mattila, A.A., Rantala, T.S., Lantto, V., and Leppävuori, S., *Sens. Actuators, B*, 1992, vol. 6, nos. 1–3, p. 248.
16. Gong, J., Chen, Q., Lian, M.R., Liu, N.C., Stevenson, R.G., and Adami, F., *Sens. Actuators, B*, 2006, vol. 114, no. 1, p. 32.
17. Ngoc, T.M., Van Duy, N., Hung, C.M., Hoa, N.D., Nguyen, H., Tonezzer, M., and Van Hieu, N., *Anal. Chim. Acta*, 2019, vol. 1069, p. 108.
18. Kolhe, P.S., Koinkar, P.M., Maiti, N., and Sonawane, K.M., *Phys. B (Amsterdam, Neth.)*, 2017, vol. 524, no. 6, p. 90.
19. Song, B.Y., Zhang, M., Teng, Y., Zhang, X.F., Deng, Z.P., Huo, L.H., and Gao, S., *Sens. Actuators, B*, 2020, vol. 307, no. 12, p. 127662.
20. Sberveglieri, G., Groppelli, S., Nelli, P., Perego, C., Valdré, G., and Camanzi, A., *Sens. Actuators, B*, 1993, vol. 15, nos. 1–3, p. 86.
21. Keshtkar, S., Rashidi, A., Kooti, M., Askarieh, M., Pourhashem, S., Ghasemy, E., and Izadi, N., *Talanta*, 2018, vol. 188, p. 531.
22. Hu, X., Zhu, Z., Chen, C., Wen, T., Zhao, X., and Xie, L., *Sens. Actuators, B*, 2021, vol. 253, p. 809.
23. Hu, Q., Zhang, W., Wang, X., Wang, Q., Huang, B., Li, Y., Hua, X., Liu, G., Li, B., Zhou, J., Xie, V., and Zhang, Z., *Sens. Actuators, B*, 2021, vol. 326, no. 6, p. 128993.
24. Shaposhnik, A., Moskalev, P., Sizask, E., Ryabtsev, S., and Vasiliev, A., *Sensors*, 2019, vol. 19, no. 5, p. 1135.

Translated by O. Zhukova